



## *Curcuma xanthorrhiza* Extract Modulates *CASP3* and *TIMP1* Expression and Regulates 8-OHdG, Collagen, and Protein Levels in UV-Induced BJ Cells

Wahyu Widowati <sup>1\*</sup>, Meilinah Hidayat <sup>1</sup>, Rita Tjokropranoto <sup>1</sup>, Dwi Nur Triharsiwi <sup>2</sup>,  
and Hanna Sari Widya Kusuma <sup>2</sup>

1. Faculty of Medicine, Maranatha Christian University, Bandung, Indonesia

2. Biomolecular and Biomedical Research Center, Aretha Medika Utama, Bandung, Indonesia

### Abstract

**Background:** Ultraviolet (UV) radiation poses a significant health risk, particularly in high-exposure regions including Indonesia, contributing to more than 1.5 million UV-related Disability-Adjusted Life Years (DALYs) globally due to its involvement in photoaging, skin cancers, and chronic inflammation. This study aimed to evaluate the *Curcuma xanthorrhiza* extract (CXE) mitigating effects against UV-induced damage in human dermal fibroblasts (BJ cells) by assessing gene expression, protein integrity, DNA damage, and collagen levels.

**Methods:** BJ fibroblasts were irradiated to UV radiation and given CXE at 3.13–12.5  $\mu\text{g/ml}$  concentrations. *TIMP1* and *CASP3* gene expression were analyzed via qRT-PCR, while total protein, 8-hydroxy-2'-deoxyguanosine (8-OHdG), and collagen content were measured using ELISA.

**Results:** CXE treatment significantly upregulated *TIMP1* and downregulated *CASP3* expression in a concentration-dependent manner, with the strongest effects showed at 12.5  $\mu\text{g/ml}$  ( $p < 0.05$ ). At the same concentration, CXE significantly restored total protein levels, reduced 8-OHdG accumulation, and preserved collagen content compared with the UV-induced control ( $p < 0.05$ ).

**Conclusion:** These findings suggest CXE exerts reparative effects against UV-induced photoaging through antioxidant, anti-apoptotic, and Extracellular Matrix (ECM) preserving mechanisms, supporting its potential as a botanical anti-aging therapy.

**Keywords:** 8-OHdG, CASP3, Collagen, Curcuma, TIMP1

**To cite this article:** Widowati W, Hidayat M, Tjokropranoto R, Triharsiwi DN, Sari Widya Kusuma H. *Curcuma xanthorrhiza* Extract Modulates *CASP3* and *TIMP1* Expression and Regulates 8-OHdG, Collagen, and Protein Levels in UV-Induced BJ Cells. Avicenna J Med Biotech 2026;18(1):48-54.

### \* Corresponding author:

Wahyu Widowati, Ph.D.,  
Faculty of Medicine, Maranatha  
Christian University, Bandung,  
Indonesia

Tel: +62 22 2012186

Fax: +62 22 2015154

### E-mail:

wahyu\_w60@yahoo.com,  
wahyu.widowati@maranatha.edu

Received: 4 Jul 2025

Accepted: 8 Oct 2025

### Introduction

Ultraviolet (UV) radiation represents a major public health concern, particularly in equatorial regions including Indonesia, where the UV index frequently exceeds 10 and can reach as high as 13.7 <sup>1</sup>. Chronic UV exposure contributes substantially to skin-related disorders such as photoaging and skin cancers, including melanoma, through mechanisms involving direct DNA damage, disruption of cell cycle regulation, and persistent inflammation <sup>2,3</sup>. Globally, UV-related diseases account for about 1.5 million Disability-Adjusted Life Years (DALYs) annually <sup>4</sup>. Despite this high risk, public awareness and sunscreen usage remain low—only about 25% of individuals recognize the dangers of UV, and many do not use sufficient sun protection in their daily routines <sup>5</sup>. This problem is further exacerbated

by lifestyle and occupational exposure, particularly among youth and outdoor workers <sup>6</sup>.

At the molecular level, UV radiation induces oxidative stress that initiates intrinsic apoptotic pathways via mitochondrial dysfunction and Caspase-3 (*CASP3*) activation, a key executor protein responsible for DNA fragmentation and cell dismantling <sup>7</sup>. Concurrently, Tissue Inhibitor of Metalloproteinase-1 (*TIMP1*), known for inhibiting Matrix Metalloproteinases (MMPs), has been identified as a modulator of apoptosis, inflammation, and Extracellular Matrix (ECM) remodelling under UV stress, potentially offering protective effects <sup>8,9</sup>.

The crosstalk between *CASP3* and *TIMP1* highlights a critical regulatory axis in UV-induced skin damage.

Furthermore, UV-B exposure generates Reactive Oxygen Species (ROS), leading to oxidative DNA lesions marked by elevated 8-hydroxy-2'-deoxyguanosine (8-OHdG), impaired antioxidant enzyme function, and the degradation of skin structural proteins<sup>10</sup>. Up-regulation of MMP-1 and MMP-9 under UV stress accelerates collagen breakdown and suppresses new collagen synthesis, contributing to wrinkle formation and reduced skin elasticity<sup>11</sup>. Antioxidant enzymes such as Superoxide Dismutase (SOD) and Catalase (CAT) also show altered expression, reflecting disrupted redox balance<sup>12</sup>. These interconnected mechanisms underscore the multifactorial nature of UV-induced skin damage and the need for effective protective strategies.

While synthetic sunscreens remain the primary means of UV protection, concerns over their long-term safety, environmental toxicity, and potential skin irritation have driven interest in natural alternatives. In this context, plant-based compounds have gained attention for their dual action as antioxidants and natural UV filters. Extracts from *Aloe vera*, green tea, *Curculigo latifolia*, and seaweeds demonstrate significant photo-protective efficacy with minimal adverse effects<sup>13-15</sup>. Notably, *Curcuma xanthorrhiza* (*C. xanthorrhiza*) (Temulawak), an Indonesian native plant, is known as a promising botanical candidate owing to its rich content of curcumin, xanthorrhizol, and essential oils. These naturally derived bioactive compounds possess anti-inflammatory, antioxidant, and anti-MMP activities that protect against UV-induced damage, support fibroblast proliferation, promote collagen integrity, and enhance wound healing and skin barrier function<sup>16-21</sup>. Therefore, the exploration of *C. xanthorrhiza* not only aligns with the pursuit of safer and more sustainable skin protection strategies but also underscores the therapeutic potential of locally sourced botanicals in combating UV-related skin damage.

Considering the UV radiation multifaceted impact in maintaining skin homeostasis and the promising *C. xanthorrhiza* properties, this study aims to evaluate *C. xanthorrhiza* Extract (CXE) efficacy by measuring key markers of skin damage and repair. Gene expression of *CASP3* and *TIMP1* was assessed using RT-PCR to investigate apoptotic activity and ECM regulation. In addition, ELISA was used to quantify 8-OHdG as an oxidative DNA damage marker, as well as total collagen and protein levels to evaluate structural integrity and overall protein preservation. These parameters provide a comprehensive view of the potential of CXE in modulating photoaging-related effects at both molecular and biochemical levels.

## Materials and Methods

### *C. xanthorrhiza* extract (CXE) preparation

PT. FAST (Fathonah Amanah Shidiq Tabligh), in Depok, Indonesia, processed and standardized the *C. xanthorrhiza* rhizome extract in compliance with Food

and Drug Authority standards [CoA No. Batch 00110201069, under Good Manufacturing Practices (GMP)]. The extract was obtained using 70% ethanol and subsequently blended with lactose to produce powdered CXE<sup>22</sup>. Although purification was not performed in our laboratory and the detailed content of bioactive compounds (e.g., curcumin, xanthorrhizol) was not quantified, standardization was assured by the supplier.

### Preparation of BJ cells

Human dermal fibroblast cells (BJ; ATCC® CRL-2522™) were acquired from Aretha Medika Utama, Indonesia. This study involved only commercially available cell lines and did not include human participants or animal subjects, ethical approval was not required. Cells were maintained in Minimum Essential Medium (MEM; Biowest, L0416-500) supplemented with Fetal Bovine Serum Premium (FBS; Biowest, S181B-500), Gentamicin (Gibco, 15750060), Antibiotic-Antimycotic (ABAM; Biowest, L0010-100), MEM Vitamins 100× (Biowest, X0556-100), Amphotericin B (Biowest, L0009-050), and MEM Non-Essential Amino Acids 100× (Biowest, X0557-100). Cells were maintained at 37°C with 5% CO<sub>2</sub> in an incubator (Thermo, IH3543)<sup>23,24</sup>.

### Treatment of CXE in UV-induced fibroblasts cells

BJ cells (1×10<sup>6</sup>) were irradiated to UV in six-well plates for 75 min at 37°C with 5% CO<sub>2</sub> using a UVP UVGL-15 lamp (Analytik Jena, Germany) positioned 15 cm above the culture plates. The lamp emitted UVA (365 nm) and UVC (254 nm), resulting in a total dose of approximately 1.23 J/cm<sup>2</sup>, which falls within the range used in previous fibroblast photoaging study<sup>25</sup>. CXE powder was initially dissolved in DMSO and diluted in culture medium to achieve 3.13, 6.25, and 12.5 µg/ml as final concentrations, with the final DMSO concentration kept below 0.1%. The tested concentrations (3.13, 6.25, and 12.5 µg/ml) were chosen based on preliminary cytotoxicity screening, which confirmed their non-toxicity to BJ cells. Following UV exposure, cells were given CXE and maintained for 24 hr before harvested for RNA and protein assays. Cells were harvested using 0.25% trypsin-EDTA (Gibco, 25200072)<sup>23</sup>. The experimental design included of five groups: I=negative control (non-irradiated cells), II=positive control (UV-induced cells without CXE treatment), III=UV-induced cells treated with CXE 3.13 µg/ml, IV=UV-induced cells treated with CXE 6.25 µg/ml, and V=UV-induced cells treated with CXE 12.5 µg/ml.

### Total protein assay

Cell pellets were washed twice with cold *Phosphate-Buffered Saline* (PBS) and lysed using RIPA buffer (Thermo Scientific, 89901) that contained protease inhibitor cocktail (Sigma-Aldrich, P8340). Lysates were centrifuged at 12,000×g for 15 min at 4°C, and the supernatants were collected for protein quantification.

Total protein levels were measured using the Bradford assay with Bovine Serum Albumin (BSA; Sigma-Aldrich, A9576, USA) as a standard. A stock solution was prepared by dissolving 2 mg of BSA in 1000 µl of double-distilled water. Serial dilutions of BSA and 20 µl of each sample were added to a microplate along with 200 µl of Quick Start Dye Reagent 1X (Bio-Rad, 5000205, USA). The plate was incubated for 5 minutes at room temperature, then absorbance was measured at 595 nm using a microplate spectrophotometer (Multiskan GO, Thermo Fisher Scientific, USA) <sup>26</sup>.

**8-OHdG and collagen assays**

The levels of 8-OHdG and collagen in the culture medium were measured using ELISA kits for human 8-OHdG (Elabscience, E-EL-0028, China) and human collagen (Elabscience, E-EL-H0869, China), following the manufacturer’s instructions. According to the manufacturer’s instructions, 8-OHdG, collagen, and protein levels were quantified in culture supernatants. The presence of 8-OHdG in the medium reflects oxidative DNA by-products released during repair processes, while collagen and proteins represent fibroblast secretion into the culture medium. Absorbance was determined at 450 nm using a microplate spectrophotometer (Multiskan GO, Thermo Fisher Scientific, USA) <sup>26</sup>. Following the instructions from the manufacturer, all analyte levels were normalized to the total protein content of the samples and expressed as ng/mg protein.

**qRT-PCR assay**

Total RNA was isolated with TRI Reagent (Zymo Research, R2050-1-200) followed by purification using the Direct-zol™ RNA Miniprep Plus Kit (Zymo Research, R2073), according to the protocols from the manufacturer. RNA purity and concentration were performed using a spectrophotometer (Multiskan GO, Thermo Scientific, 51119300) by measured the absorbance at 260 and 280 nm (Table 1). Complementary DNA (cDNA) was synthesized from the extracted RNA using the SensiFAST cDNA Synthesis Kit (Bio-line, BIO-65054) through primer annealing, reverse

transcription, and enzyme deactivation <sup>23</sup>. Quantitative PCR was carried out using the AriaMx RT-PCR System (Agilent, G8830A). The cycling protocol contained initial denaturation for 5 min at 95°C, followed by 40 amplification cycles including denaturation for 50 s at 95°C, annealing at gene-specific temperatures (55-58°C, Table 1), and elongation at 72°C for 50 s. Melt-curve analysis was conducted at the end of each run to verified the specificity of amplification. Amplification efficiencies ranged from 90-100%, which is within the acceptable range for qRT-PCR assays. *β-actin* was employed as the internal control. The primers employed for real-time PCR are presented in table 2.

**Statistical analysis**

Statistical analysis was assessed using SPSS version 23.0 (SPSS Inc., USA). All data are represented as mean±Standard Deviation (SD) (n=3). The Shapiro–Wilk test was employed to evaluate data normality, while Levene’s test assessed variance homogeneity. Normally distributed and homogeneous data were analyzed with one-way ANOVA followed by Tukey’s HSD post hoc test. For data that were not normally distributed but not homogeneous, the Mann–Whitney post hoc test was used. A p<0.05 was considered statistically significant. Data visualization was performed in histogram format using GraphPad Prism software (version 8.0.244) <sup>23,26</sup>.

**Results**

**Effect of various CXE concentrations toward CASP3 and TIMP1 genes expression in UV-induced BJ cells**

Gene expression analysis of *TIMP1* and *CASP3* in UV-induced BJ cells given with CXE is presented in figure 1. UV irradiation significantly altered both genes expression compared with the negative control group (I). *TIMP1* mRNA expression was markedly increased in the positive control group (II) relative to the negative control (I) shown in figure 1A, which showed the lowest expression. This likely reflects the absence of oxidative stress or extracellular matrix remodelling

Table 1. Purity and concentration of RNA

Sample	Purity (λ260/ λ280 nm)	Concentration (ng/µl)
BJ cells (negative control)	2.3243	354.20
UV-induced BJ cells (positive control)	2.3260	335.60
UV-induced cells treated with CXE 3.13 µg/ml	2.3240	288.00
UV-induced cells treated with CXE 6.25 µg/ml	2.3975	252.30
UV-induced cells treated with CXE 12.5 µg/ml	2.3599	165.50

Table 2. Gene primer sequences employed in this study

Gene (human)	Primer sequence (5’–3’)	Annealing temp (°C)	Product size (bp)
<i>β-actin</i>	F: TCT-GGC-ACC-ACA-CCT-TCT-ACA-ATG R: AGC-ACA-GCC-TGG-ATA-GCA-ACG	58	142
<i>TIMP1</i>	F: AGT-CAA-CCA-GAC-CAC-CTT-ATA-CCA R: TTT-CAG-AGC-CTT-GGA-GGA-GCT-GGT-C	58	138
<i>CASP3</i>	F: CTG-GTT-TTC-GGT-GTT-TGT R: CAG-TGT-TCT-CCA-TGG-ATA-CCT-TTA-TT	55	150

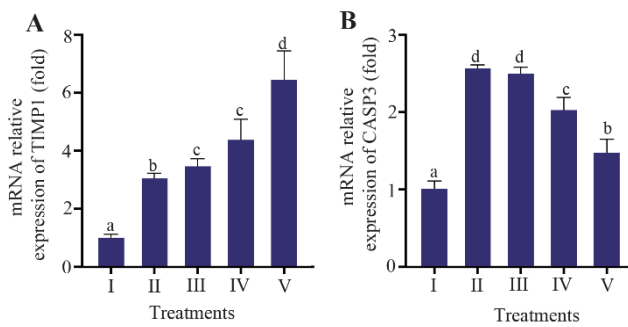


Figure 1. Effect of CXE on *TIMP1* and *CASP3* gene expression in UV-induced BJ cells.

Relative mRNA expression of (A) *TIMP1* and (B) *CASP3* in BJ cells. Groups: I=NC (Negative Control, non-irradiated), II=PC (Positive Control; UV-induced), III=PC+CXE 3.13  $\mu\text{g/ml}$ , IV=PC+CXE 6.25  $\mu\text{g/ml}$ , and V=PC+CXE 12.5  $\mu\text{g/ml}$ . Data are represented as mean $\pm$ SD (n=3). Statistical significance was determined using the Mann-Whitney test. Bars labelled with different letters indicate statistically significant differences between groups ( $p < 0.05$ ).

in non-irradiated cells. Treatment with CXE at increasing concentrations (III–V) resulted in a progressive and significant upregulation of *TIMP1*, with the highest expression was observed at 12.5  $\mu\text{g/ml}$  (V) ( $p < 0.05$ ).

In contrast, *CASP3* expression followed a different trend (Figure 1B). UV exposure (II) significantly upregulated *CASP3* expression compared with the negative control. Treatment with CXE modulated this response.

Although expression levels remained elevated in groups III and IV (3.13 and 6.25  $\mu\text{g/ml}$ ), the highest concentration (12.5  $\mu\text{g/ml}$ ; group V) significantly reduced *CASP3* expression relative to the positive control ( $p < 0.05$ ). These findings highlight that CXE may possess anti-apoptotic effects at higher concentrations.

#### Effect of various CXE concentrations on total protein, 8-OHdG, and collagen levels in UV-induced BJ cells

Treatment with CXE demonstrated significant effects on total protein content, oxidative DNA damage, and collagen levels in UV-induced BJ cells. UV exposure reduced total protein levels compared with non-irradiated cells. However, CXE treatment at 12.5  $\mu\text{g/ml}$  (V) significantly restored total protein levels relative to the positive control, indicating improved cellular integrity under oxidative stress conditions (Figure 2A). 8-OHdG levels, a marker of oxidative DNA damage, were markedly elevated after UV induction. Treatment with CXE resulted in a concentration-dependent decrease in 8-OHdG levels, both in absolute values ( $\mu\text{g/ml}$ ) and normalized to protein ( $\text{ng/mg}$  protein), with the greatest reduction observed at 12.5  $\mu\text{g/ml}$  (V) (Figures 2B and 2C). Values in Figure 2C were obtained by dividing the concentrations shown in figure 2B by the corresponding total protein levels of the negative control.

UV exposure also caused a notable decline in collagen levels. However, CXE treatment helped reverse this effect, with the highest concentration (12.5  $\mu\text{g/ml}$ ;

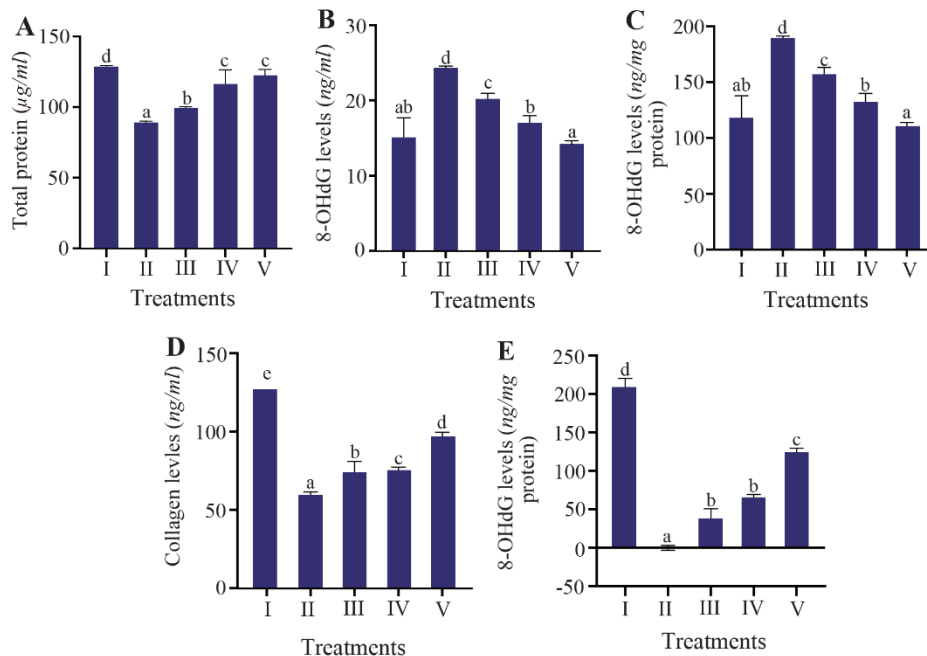


Figure 2. Effect of CXE on protein level, oxidative DNA damage, and collagen content in UV-induced BJ cells. A) total protein ( $\mu\text{g/ml}$ ); B) 8-OHdG ( $\text{ng/ml}$ ); C) 8-OHdG normalized to total protein ( $\text{ng/mg}$  protein); D) collagen ( $\text{ng/ml}$ ); E) collagen normalized to total protein ( $\text{ng/mg}$  protein). Groups: I=NC (Negative Control, non-irradiated), II=PC (Positive Control; UV-induced), III=PC+CXE 3.13  $\mu\text{g/ml}$ , IV=PC+CXE 6.25  $\mu\text{g/ml}$ , and V=PC+CXE 12.5  $\mu\text{g/ml}$ . Data are presented as mean $\pm$ SD (n=3). Statistical analysis was conducted using one-way ANOVA followed by Tukey's HSD post hoc test for normally distributed and homogeneous data (Figures 2D–E), and the Mann-Whitney U test for non-normal and non-homogeneous data (Figures 2A–C). Bars labelled with different letters indicate statistically significant differences between groups ( $p < 0.05$ ).

V) significantly increased collagen content in both *ng/ml* and *ng/mg* protein measurements. This suggests enhanced extracellular matrix preservation and potential anti-photoaging properties (Figures 2D and 2E). Figure 2E were obtained by dividing the concentrations in figure 2D by the total protein of the negative control.

### Discussion

This study provides evidence that CXE exerts multifaceted protective effects against UV-induced damage in fibroblasts. The significant upregulation of *TIMP1* observed in UV-induced BJ cells treated with CXE, particularly at 12.5  $\mu\text{g/ml}$ , suggests a potential anti-aging mechanism through ECM protection. Elevated *TIMP1* in UV-induced cells may represent a defensive response to oxidative stress, while its further enhancement by CXE indicates amplification of this protective mechanism. In non-irradiated cells (negative control), *TIMP1* expression remained low, reflecting the absence of extracellular matrix remodelling or oxidative stress. In contrast, UV irradiation markedly increased *TIMP1* levels in the positive control group, consistent with previous reports that *TIMP1* is upregulated under oxidative and inflammatory stress to counteract MMP activity and support cell survival<sup>9,27</sup>. *TIMP1* contributes in maintaining ECM homeostasis by inhibiting MMPs, which are implicated in collagen degradation during photoaging<sup>27</sup>. Additionally, CXE's bioactive components such as curcumin and xanthorrhizol may modulate inflammatory and oxidative pathways, contributing to increased *TIMP1* expression<sup>28</sup>. This response not only limits ECM breakdown but also supports fibroblast survival and functional stability under stress<sup>29</sup>. Collectively, these results position CXE as a potential agent for reinforcing ECM integrity in UV-stressed skin.

The treatment of CXE also modulated apoptotic signaling, particularly *CASP3*. UV exposure significantly increased *CASP3* expression, reflecting enhanced apoptotic stress. However, this was mitigated at higher CXE concentrations, indicating a protective, anti-apoptotic effect. These findings align with previous reports of curcumin's antioxidant activity, which helps reduce ROS accumulation and apoptosis in non-cancerous cells<sup>30</sup>. CXE appears to regulate cell death more conservatively that may involve modulation of PI3K/AKT or NF- $\kappa$ B pathways to support cell survival<sup>31</sup>, further reinforcing CXE's role in maintaining skin cell viability.

CXE treatment also restored total protein levels in UV-induced fibroblasts. UV irradiation reduced protein content, likely due to increased degradation and decreased biosynthesis. However, CXE, especially at 12.5  $\mu\text{g/ml}$ , significantly recovered protein levels, suggesting improved cellular metabolism and resilience. Prior studies have shown that curcumin enhances expression of protective proteins like SIRT1 and down-regulates MMP-1, aiding ECM preservation and fibro-

blast proliferation<sup>18,32</sup>. These actions collectively suggest that CXE helps maintain structural proteins critical for skin integrity under stress.

A key marker of oxidative DNA damage, 8-OHdG, was significantly elevated following UV exposure but reduced with CXE treatment in a concentration-dependent manner. This reduction highlights the strong antioxidant properties of CXE in neutralizing ROS and preventing DNA lesions. Similar reductions in oxidative stress markers have been reported with other Curcuma-based treatments<sup>33</sup>. Furthermore, studies by Anggayanti *et al* reported that CXE enhances fibroblast proliferation, vascularization, and ECM synthesis, all of which support contributed to improved resilience and reduced oxidative burden<sup>34</sup>. By restoring redox balance, CXE may enhance fibroblast longevity and functionality under prolonged UV stress<sup>34</sup>.

CXE also preserved collagen, a major ECM component degraded during photoaging. UV exposure increases MMP-1 and accelerates collagen degradation, but CXE counteracted this effect and significantly restored collagen levels. This finding is consistent with earlier study showing that curcumin inhibits MMP expression and stimulates collagen biosynthesis pathways<sup>35</sup>. The TGF- $\beta$  pathway involvement in enhancing collagen production and ECM stability may explain the observed improvement in structural integrity<sup>36</sup>. These effects highlight CXE's promise in supporting skin regeneration and resilience.

The molecular actions of CXE suggest a multifaceted cytoprotective effect against UV-induced fibroblast damage. By upregulating *TIMP1* and preserving collagen, CXE maintains ECM architecture<sup>37</sup>. Down-regulation of *CASP3* supports fibroblast survival by inhibiting apoptotic cascades<sup>38</sup>. Enhanced protein content and decreased 8-OHdG levels indicate improved biosynthetic capacity and DNA protection, likely mediated by antioxidant pathways<sup>25</sup>. These coordinated mechanisms converge to maintain fibroblast function and structural integrity under oxidative stress, underscoring the therapeutic potential of CXE as a botanical anti-aging agent.

This study has several limitations. It focused only on *CASP3* and *TIMP1* as representative apoptotic and ECM-related markers, without including others such as BAX, BCL-2, and p53. Detailed phytochemical profiling of the extract, including quantification of curcumin and xanthorrhizol, was not conducted. The absence of a vehicle control for DMSO and a positive control with a known photoprotective agent also limits interpretation, although the final DMSO concentration ( $\leq 0.1\%$ ) is generally non-toxic to fibroblasts. Analyses were performed with three biological replicates, which may reduce statistical power. Other indicators of UV-induced damage, such as intracellular free radical generation and senescence-associated  $\beta$ -galactosidase activity, were not assessed. Finally, UV irradiation was performed in the presence of medium, which may

attenuate penetration and lower the effective dose. Future studies should optimize UV exposure conditions, quantify medium transmission, expand the panel of apoptotic, oxidative stress, and senescence markers, include solvent and standard controls, perform detailed phytochemical characterization, and use larger sample sizes to strengthen the conclusions and provide a more comprehensive understanding of the photoprotective potential of CXE.

### Conclusion

*C. xanthorrhiza* Extract (CXE) demonstrated significant mitigating effects against UV-induced damage in BJ fibroblasts through the modulation of molecular markers. CXE upregulated *TIMP1* expression while downregulating *CASP3*, indicating its roles in maintaining extracellular matrix integrity and reducing apoptosis. Additionally, CXE treatment restored total protein levels, reduced oxidative DNA damage (8-OHdG), and preserved collagen content. These findings highlight the potential of CXE for combating photoaging by promoting cellular resilience and attenuating oxidative stress. Future studies should investigate the in vivo efficacy and molecular mechanisms of CXE to support its development as a topical anti-aging agent.

### Acknowledgement

The authors acknowledge the financial support provided by Maranatha Christian University.

### Conflict of Interest

No conflicts of interest are declared by the authors.

### References

- Kaiser I, Pfahlberg A, Lehmann M, Buchta E, Uter W, Gefeller O. The extent of public awareness and use of the global solar UV index as a worldwide health promotion instrument to improve sun protection: a systematic review and meta-analysis. *Photochem Photobiol* 2024;101(3):636-659.
- Silva V, Wang X, Montelpare W, Kmay P. A literature review of climate change-related risk factors for cancer development. *Environ Res Health* 2025;3:022003.
- Neale R, Lucas R, Byrne S, Hollestein L, Rhodes L, Yazar S, et al. The effects of exposure to solar radiation on human health. *Photochem Photobiol Sci* 2023;22(5):1011-1047.
- Tikle S, Beig G. Is ultraviolet radiation a confounding variable for COVID-19 in India?. *J ISAS* 2022;1(1):123-137.
- Janka E, Ványai B, Dajnoki Z, Szabó I, Reibl D, Komka I, et al. Regional variability of melanoma incidence and prevalence in Hungary. Epidemiological impact of ambient UV radiation and socioeconomic factors. *Eur J Cancer Prev* 2021;31(4):377-384.
- Mahmoodpour S, Shoostari L, Rafiefard N, Mohamadpour R, Taghavinia N, Vashae D. Scalable and cost-effective fabrication of high-performance self-powered heterojunction UV-photodetectors using slot-die printing of triple-cation lead perovskite coupled with triboelectric nanogenerators. *J Phys Energy* 2023;6(1):015014.
- He Y, Zheng X, Hu Y, Deng L, Xu J, Wu S. Proteomics analysis to investigate the potential mechanism of theacrine against UV-induced skin photodamage. *Photodermatol Photoimmunol Photomed* 2023;39(6):620-632.
- Tchetina E, Glemba K, Markova G, Naryshkin E, Тацкина Е, Макаров М, et al. Development of postoperative pain in patients with end-stage knee osteoarthritis is associated with upregulation of genes related to extracellular matrix degradation, inflammation, and apoptosis. *Life (Basel)* 2020;10(10): 224.
- Ma B, Ueda H, Okamoto K, Bando M, Fujimoto S, Okada Y, et al. TIMP1 promotes cell proliferation and invasion capability of right-sided colon cancers via the FAK/AKT signaling pathway. *Cancer Sci* 2022;113(12): 4244-4257.
- Cho E, Ahn S, Shin K, Lee J, Hwang H, Choi Y. Protective effect of red light-emitting diode against UV-B radiation-induced skin damage in SKH:HR-2 hairless mice. *Curr Issues Mol Biol* 2024;46(6):5655-5667.
- Lee Y, Jeong D, Jeun Y, Choe H, Yang S. Preventive and ameliorative effects of potato exosomes on UVB induced photodamage in keratinocyte HaCaT cells. *Mol Med Rep* 2023;28(3):1-10.
- Hoskin R, Pambianchi E, Pecorelli A, Grace M, Therrien J, Valacchi G, et al. Novel spray dried algae-rosemary particles attenuate pollution-induced skin damage. *Molecules* 2021;26(13):3781.
- Sharma M. Understanding the impact of UV radiation on skin health: mechanisms, risks, and photoprotection strategies. *Indian J Health Care Med Pharm Pract* 2024; 5(1): 88-95.
- Karagöz I, Simitcioglu B. Ex vivo UV-C protective effect of Aloe vera. *Bitlis Eren Univ Sci J* 2024;13(1):23-29.
- Nur S, Hanafi M, Setiawan H, Elya B. In vitro ultra violet (UV) protection of curculigo latifolia extract as a sunscreen candidate. *InIOP Conference Series: Earth and Environmental Science* 2022 Dec 1 (Vol. 1116, No. 1, p. 012009). IOP Publishing.
- Minarni M, Asyhar R, Juliana D, Yudha YS, Nurcholis W. Analysis of rhizome color and phytochemical content of 10 accessions of *Curcuma xanthorrhiza* Roxb. in Jambi, Indonesia. *Biodiversitas Journal of Biological Diversity*. 2023 Jan 18;24(1).
- Alolga R, Wang F, Zhang X, Li J, Tran L, Yin X. Bioactive compounds from the Zingiberaceae family with known antioxidant activities for possible therapeutic uses. *Antioxidants* 2022;11(7):1281.
- Pabuprapap W, Nakyai W, Chaichompoo W, Pheedee N, Phetkeereerat S, Viyoch J, et al. *Curcuma aromatica* and *Curcuma comosa* extracts and isolated constituents provide protection against UVB-induced damage and attenuate MMP-1 expression in HaCaT cells. *Cosmetics* 2022; 9(1):23.
- Rahmat E, Lee J, Kang Y. Javanese turmeric (*Curcuma xanthorrhiza*): ethnobotany, phytochemistry, biotechno-

- logy, and pharmacological activities. *Evid Based Complement Alternat Med* 2021;2021:9960813.
20. Barbalho S, Gonzaga H, Souza G, Goulart R, Gonzaga M, Rezende B. Dermatological effects of *Curcuma* species: a systematic review. *Clin Exp Dermatol* 2021; 46(5): 825-833.
  21. Marini M, Priatni H, Darotulmutmainnah A, Safitri D. Physical evaluation of *Curcuma* rhizome extract (*Curcuma xanthorrhiza*) formulation in anti-acne loose powder. *Med Sains J Ilm Kefarmasian* 2023;8(2):871-878.
  22. Darsono L, Widowati W, Lucianus J, Setiabudi E, Obeng SS, Stefani S, et al. The ethanolic extract of *Clitoria ternatea* attenuates SMADs and REGs regulation in dyslipidemia and diabetes mellitus rat model. *Nat Prod Sci* 2023;29(4):193-199.
  23. Widowati W, Dani D, Vera V, Wargasetia TL, Rahardja F, Tih F, Hadiprasetyo DS. *Salacca zalacca* extract's antiaging effect on aging genes, protein levels, and apoptosis in UV-induced fibroblast cells. *J Taibah Univ Med Sci* 2025;20(3): 349-358.
  24. Girsang E, Lister I, Ginting CN, Widowati W, Arumwardana S, Marthania M, et al. Chlorogenic acid in preventing and curing ultraviolet-induced damage in human skin fibroblast as an antiaging cell model. *Pharmaciana* 2023;13:159-165.
  25. Yang C, Rybchyn M, Silva W, Matthews J, Holland A, Conigrave A, et al. UV-induced DNA damage in skin is reduced by CaSR inhibition. *Photochem Photobiol* 2022; 98(5):1157-1166.
  26. Widowati W, Tjokropranoto R, Onggowidjaja P, Kusuma HSW, Wijayanti CR, Marthania M, et al. Protective effect of *yacon* leaves extract through antifibrosis, anti-inflammatory, and antioxidant mechanisms toward diabetic nephropathy. *Res Pharm Sci* 2023;18(3):336-345.
  27. Xiao W, Wang L, Howard J, Kolhe R, Rojiani A, Rojiani M. TIMP-1-mediated chemoresistance via induction of IL-6 in NSCLC. *Cancers (Basel)* 2019;11(8):1184.
  28. Marni M, Firdaus I, Wahyuningsih W, Soares D, Raharja M, Savitri D. Effectiveness of honey, *Curcuma* and turmeric for child health: a literature review. *Proc Int Conf Sci Health Technol* 2023;4:444-450.
  29. Schoeps B, Eckfeld C, Flüter L, Keppler S, Mishra R, Knolle P, et al. Identification of invariant chain CD74 as a functional receptor of TIMP-1. *J Biol Chem* 2021; 297(3):101072.
  30. Widyastuti I, Luthfah H, Hartono Y, Islamadina R, Can A, Rohman A. Antioxidant activity of *temulawak* (*Curcuma xanthorrhiza*) and its classification with chemometrics. *Indones J Chemom Pharm Anal* 2020;29(3):28-41.
  31. Venkatesan K, Sivadasan D, Weslati M, Gayasuddin M, Goyal M, Bansal M, et al. Protective effects of frankincense oil on wound healing: downregulating caspase-3 expression to facilitate the transition from the inflammatory to proliferative phase. *Pharmaceuticals (Basel)* 2025; 18(3):407.
  32. Prasetyawan S, Safitri A, Atho'llah M, Rahayu S. Computational evaluation of bioactive compounds in *Curcuma xanthorrhiza* targeting SIRT1 and NF- $\kappa$ B. *Biotechnology* 2023;104(2):171-182.
  33. Rosidi A, Ayuningtyas R, Jauharany F, Ekasari S, Millah A, Fauziah S, et al. Pre-exercise supplementation with *Curcuma xanthorrhiza* has minimal impact on red blood cell parameters but reduces oxidative stress: a preliminary study in rats. *Phys Act Nutr* 2024;28(3):52-57.
  34. Anggayanti N, Sudirman P, Paramita M. Effectivity of 5% *temulawak* extract on post-extraction fibroblast cells in Wistar rats. *Padjadjaran J Dent* 2023;35(2):151-5.
  35. Lorenzo R, Grumetto L, Sacchi A, Laneri S, Dini I. Dermocosmetic evaluation of a nutricosmetic formulation based on *Curcuma*. *Phytother Res* 2022;37(5):1900-1910.
  36. Ham S, Song M, Yoon H, Lee D, Chung J, Lee S. SPARC is highly expressed in young skin and promotes extracellular matrix integrity in fibroblasts via the TGF- $\beta$  signaling pathway. *Int J Mol Sci* 2023;24(15):12179.
  37. Hong L, Chen X, Zhu M, Ao Z, Tang W, Zhou Z. TIMP1 may affect goat prolificacy by regulating biological function of granulosa cells. *Arch Anim Breed* 2022; 65(1):105-111.
  38. Abe K, Yamamoto K, Myoda T, Fujii T, Niwa K. Protective effects of volatile components of aged garlic extract against UVB-induced apoptosis in human skin fibroblasts. *J Food Biochem* 2022;46(12):e14482.